Photoswitchable Diazocine-based Estrogen Receptor Agonists Stabilization of the Active Form Inside the Receptor

Julia Ewert [1,‡], Linda Heintze [2,‡], Mireia Jordà-Redondo [3], Jan-Simon von Glasenapp [1], Santi Nonell [3], Götz Bucher [4], Christian Peifer [2,*] and Rainer Herges [1,*]

[1]Otto-Diels-Institute of Organic Chemistry, Christian-Albrechts-University of Kiel, 24098 Kiel, Germany

[2]Institute of Pharmacy, Christian-Albrechts-University of Kiel, 24118 Kiel, Germany

[3] Institut Químic de Sarrià, Universitat Ramon Llull, 08017 Barcelona, Spain

[4] School of Chemistry, University of Glasgow, Glasgow G12 8QQ, United Kingdom

Photoswitchable Estrogene Receptor Agonists, Photoswitchable Hormones, Azobenzene/Phenylhydrazone based Tautomerization

ABSTRACT: Photopharmacology is an emerging approach in drug design and pharmacological therapy. Light is used to switch a pharmacophore between a biologically inactive and an active isomer with high spatiotemporal resolution at the site of illness, thus, potentially avoiding side effects in neighboring healthy tissue. The most frequently-used strategy to design a photoswitchable drug is to replace a suitable functional group in a known bioactive molecule with azobenzene. Our strategy is different in that the photoswitch moiety is closer to the drug´s scaffold. Docking studies reveal a very high structural similarity of natural 17β-estradiol and the *E* isomers of dihydroxy diazocines, but not their *Z* isomers, respectively. Seven dihydroxy diazocines were synthesized and subjected to a biological estrogen reporter gene assay. Four derivatives exhibit distinct estrogenic activity after irradiation with violet light, which can be shut off with green light. Most remarkably, the photogenerated, active *E* form of one of the active compounds isomerizes back to the inactive *Z* form with a half-life of merely several ms in water, but nevertheless is active for more than 3 h in the presence of the estrogen receptor. The results suggest a significant local impact of the ligand-receptor complex towards back-isomerization. Thus, drugs that are active when bound, but lose their activity immediately after leaving the receptor could be of great pharmacological value because they strongly increase target specificity. Moreover, the drugs are released into the environment in their inactive form. The latter argument is particularly important for drugs that act as endocrine disruptors.

Introduction

Site specific, targeted drug therapy avoids unwanted side effects in neighboring, healthy tissue.[1,2] Photoswitchable drugs are a particularly promising approach towards this end.[3–9] Preferentially, the switchable drug is administered in its thermodynamically stable but biologically inactive form. Depending on the rate of blood flow, blood tissue partition and other parameters, the inactive drug is more or less equally distributed within the body. Irradiation with light of suitable wavelengths at the site of interest (e.g. tumor, metastasis, inflammation) converts the drug locally into its active form. Since light can be applied with significant spatiotemporal resolution, pharmacological action is highly targeted. In an ideal photoswitchable drug the bioactive isomer is the metastable state, which slowly reverts to the stable bio-inactive form. If these drugs are excreted e.g. via the kidney, they would not be released into the environment in their active form.[2,10,11] Estrogen active compounds are of major concern in this regard.[12–15]

17β-Estradiol is the natural hormone binding to the estrogen receptors ERα and ERβ, controlling a plethora of physiological functions.[16–19] Artificial estrogen receptor binding drugs are used as contraceptives (e.g. ethinylestradiol), for the treatment of breast cancer (tamoxifen, fulvestrant etc.) and prostate cancer (raloxifene, diethylstilbestrol).[20–23] The hitherto known estrogen receptor modulators cover a surprisingly broad structural range, however, predominantly include a stilbene unit and at least one phenolic OH group (Figure 1a).[24]

A number of photoswitches, such as azobenzenes, spiropyrans, diarylethenes and diazocines have been used to design light-switchable drugs and hormones.[25–27] Diazocines stand out because of the bathochromic switching wavelengths (400 - 700 nm)[28], high switching efficiencies (60-95%),[29] very high quantum yields (70-90%)[29] and excellent fatigue resistance.[30] Most importantly, and in contrast to the frequently used azobenzenes, diazocines are stable in their bent *Z* configuration and less stable in their stretched *E* configuration (Figure 1b).[9,30,31]

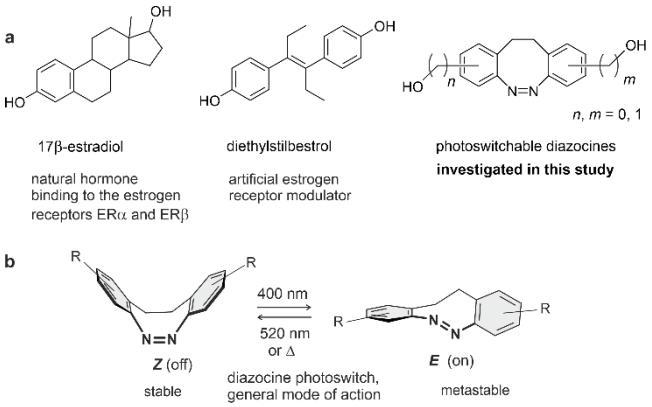

Figure 1. a) Structural comparison of 17β-estradiol, diethylstilbestrol and the designed dihydroxydiazocines b) Reversible diazocine photoswitching between the biological inactive *Z* configuration (off) and the biological active *E* configuration (on).

In the majority of cases, the less hindered *E* configuration binds to the receptor.[9] Hence, diazocine-based drugs can be administered in their inactive *Z* configuration and activated by light at the site of illness, whereas most azobenzene-based drugs exhibit the reverse mode of action. To date, several diazocine based photoswitchable, bioactive compounds have been designed and published, providing strong evidence for the use of the diazocine core in photoresponsive applications.[32–41]

Given these potentially beneficial photochemical features of the diazocine scaffold, we aimed at designing compounds where the photoswitching diazocine moiety is actually incorporated into the pharmacophore itself. By screening known bioactive compounds with diazocine-like and particularly tricyclic and tetracyclic druglike structures,[42] we came across the steroid scaffold of estrogen as a suitable model system. In this context, azobenzene-based photoswitchable estrogen receptor ligands were recently reported by Tsuchiya and Umeno *et al.*[43] Furthermore, other photoswitchable nuclear receptor ligands targeting retinoic acid receptor α, farnesoid X receptor and peroxisome proliferator-activated receptor α and γ, respectively, were published by the Trauner group recently.[26,27,44,45] In our present study, we focused on functionalized diazocines and firstly performed molecular modelling to establish a respective hypothesis. Thus, superposition of 17β-estradiol with the *meta*-dihydroxy functionalized diazocine **1** suggested the *E* configuration to resemble 17β-estradiol in molecular shape, whereas the *Z* configuration of **1** showed significantly less similarity (Figure 2a/b). Furthermore, docking of **1** in the *E* configuration within the active site of the estrogen receptor revealed a binding mode highly comparable to the original binding pose of 17β-estradiol addressing a similar ligand-protein interaction pattern (pdb 1ERE[46], Figure 2c; respective 2D-ligand-interaction-diagramm Figure 2e). In contrast, modelling of diazocine **1** in the *Z* configuration did not reveal a plausible binding pose and demonstrated severe clashes at the bottom of the estrogen receptor binding pocket. Moreover, the key H-bond interaction from the phenolic moiety to histidine 524 is missing (Figure 2d)

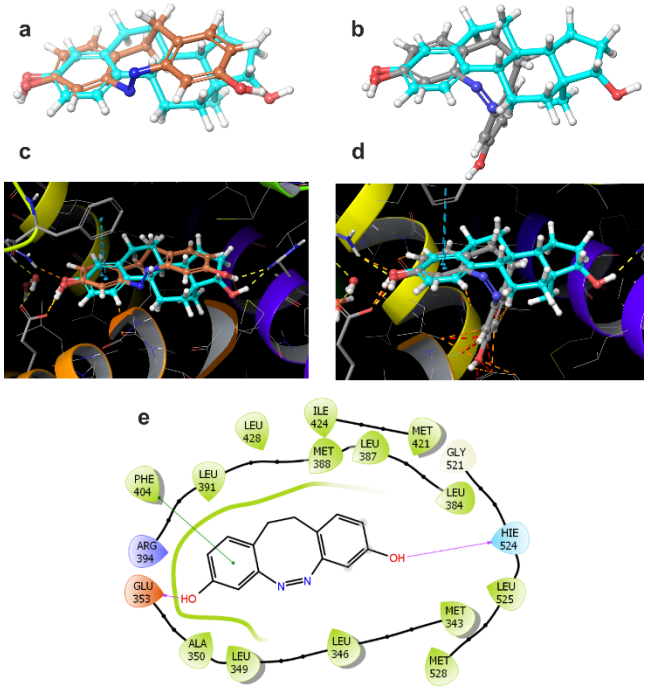

Figure 2. Molecular Modelling of diazocine **1** in *E* and *Z* configuration (*E*-**1** and *Z*-**1**) in the estrogen α receptor binding pocket (pdb 1ERE[46]). Coloring: natural substrate 17β-estradiol: light blue, *E*-**1**: brown, *Z*-**1**: grey. **a** and **c**: superposition of 17β-estradiol in the original bioactive pose with *E*-**1** showing significant molecular similarity in contrast to *Z*-**1** (**b** and **d**) producing steric clashes in the binding pocket. The respective 2D ligand-interaction diagram (**e**) illustrates key interactions of *E*-**1** within the binding site.

Results and Discussion

Based on the hypothesis supported by docking studies that dihydroxy diazocines could be used as photoswitchable estrogens, we set out to design, synthesize and photochemically characterize a set of promising diazocine derivatives with substitutions in *meta*- and *para*-position to the azo group and benzylic hydroxyl moieties (compounds **1** - **7**, Figure 3). Having the compounds in hand, we analyzed their photophysical properties and characterized their photoresponsive effects in a cell based estrogen reporter gene assay.

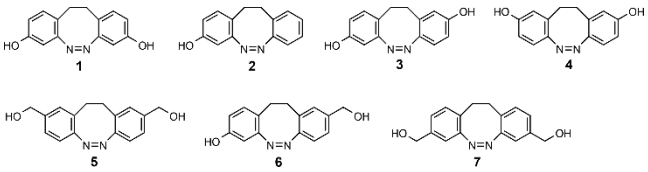

Figure 3. (Di)hydroxy diazocines **1** - **7** investigated in this study.

Synthesis

The difunctionalized diazocines **1** and **3** - **6** were synthesized following previously published strategies for the preparation of diazocines. These approaches are based on oxidative C-C couplings of nitrotoluenes derivatives followed by reductive azo cyclization (Scheme 1).[47–49] The previously published *meta*-

benzyl alcohol diazocine **7** was synthesized by Moormann *et al*.[49]

In order to investigate the influence of the hydroxy groups on estrogenic activity in comparison to the difunctionalized diazocine based estrogen receptor ligands, we also prepared the monosubstituted hydroxy-diazocine **2** via a Wittig reaction approach followed by an oxidative cyclization (Scheme 1).[33,41,50,51] For more experimental details see Supporting Information Section 3.

Scheme 1. Synthesis of dihydroxy diazocines 1, 3 - 6 and monohydroxy diazocine 2

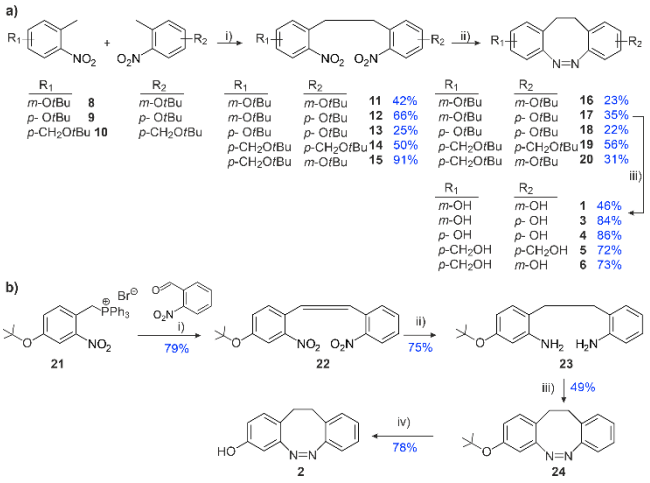

a) Reaction conditions: (i) 1.) KO*t*Bu, THF, -5°C; 2.) Br_2, THF, rt.; (ii) 1.) $Ba(OH)_2$, Zn, EtOH, H_2O, reflux; 2.) $CuCl_2$, O_2, MeOH, 0.1 M NaOH, rt.; (iii) $TiCl_4$, DCM, 0 °C; conditions for compound **1** and **4**: TFA, DCM, rt. **b)** Reaction conditions: (i) KO*t*Bu, THF, 10 min reflux, 50 °C; (ii) H_2, Pd/C rt.; (iii) Oxone, DCM/H_2O (1:1), rt.; (iv) $TiCl_4$, DCM, 0 °C.

Photochemical Characterization

The photochemical properties of the diazocines **1** - **7** were examined both in DMSO and in aqueous solution. The data served as a basis to choose the conditions for the biological assay (at 25°C and 37°C). The optimal excitation wavelengths for the *Z*→*E* isomerization and half-lives ($t_{½}$) of the *E* isomers of compounds **1** - **7** were determined by UV/Vis absorption spectroscopy and nanosecond laser flash photolysis. Additionally, photostationary states (PSS) were measured using ^{1}H-NMR spectroscopy (for ^{1}H-NMR spectra of all compounds, see SI Section 4.3). All results are summarized in Table 1. The absorption maxima of the n-π* bands of the *Z* isomers are between 403 nm and 414 nm in DMSO. Upon irradiation at 385 nm (optimal excitation wavelength for compound **5** – **7**) or 405 nm (optimal switching wavelength for compound **1** - **4**) the *E* isomers are formed, which exhibit absorption maxima of the n-π* excitation in a range between 487 nm and 497 nm. The back-isomerization is quantitative upon irradiation with 530 nm (green light).

In Figure 4, UV/Vis absorption spectra of diazocines **3** and **6** in DMSO are shown exemplary (for UV/Vis spectra of all compounds, see SI Figure S1). In the special case of the *para*-substituted hydroxy diazocines **3** and **4** a small absorption band emerges at 606 nm and 608 nm, respectively. This band can be assigned to the hydrazo isomer, which is formed by an azobenzene/phenylhydrazone tautomerism. An analogous tautomerization process has been previously observed in *para*-hydroxy azobenzene.[52–54]

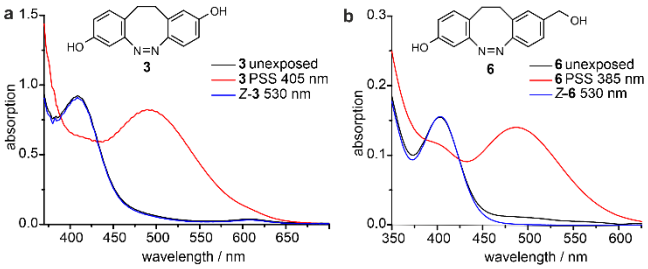

Figure 4. UV/Vis spectra of the diazocines **3** and **6** in DMSO at 25 °C. The spectra of the unexposed samples are plotted in black and the PSS spectra after irradiation with 385 nm/ 405 nm are shown in red. The *Z* isomers after irradiation with 530 nm are plotted in blue. a) UV/Vis spectra of the hydroxy diazocine **3** (1.1 mM). b) UV/Vis spectra of diazocine **6** (200 µM).

The photostationary states of the hydroxy diazocines **1** - **7** after irradiation with 385 or 405 nm in DMSO are between 43 % and 83 % (*E* isomer). The photochemical back-reaction with green light is quantitative (>99%, Table 1). The thermal back-isomerization processes (*E* → *Z*) were measured by UV spectroscopy and the data were fitted to first-order kinetics (UV/Vis spectra and linear fits in DMSO and water for all compounds, see SI Section 4.2). The half-lives ($t_{1/2}$) of compound **1** - **2** and **5** - **7** vary from 4.0 h to 12.7 h in DMSO (Table 1), which is in the range of the parent diazocine and a number of substituted systems.[49] With $t_{1/2}$ = 2.4 min and 19.9 s, the *E* isomers of **3** and **4** exhibit shorter half-lives (Table 1). At higher concentrations, deviations from first order kinetics were observed for diazocine **3** (for the first-order kinetic fit, see SI Figure S22).

In water the n-π* absorption maxima of the *E* and *Z* isomers are shifted hypsochromically. The n-π* absorptions of the *Z* isomers are located at 396 nm ($\Delta\lambda_{max}$~-14 nm), while the n-π* absorptions of the *E* isomers shift to a larger extent to 471 nm ($\Delta\lambda_{max}$~-21 nm), resulting in a lower band separation (for UV/Vis spectra in water, see SI Figure S2). Consequently, in aqueous media the PSS values of the diazocines **1** - **2** and **5** - **7** decrease, while the half-lives (*E* → *Z*) approximately triple with respect to the values in DMSO ($t_{1/2}$ (H_2O): 15.2 – 42.4 h). As expected, the half-lives decrease again at higher temperatures (37°C), but still remain in the range of hours (9.6 – 4.5 h, Table 1). A dramatical change, however, is observed for the half-lives of the *E* isomers of compounds **3** and **4**, which are susceptible to tautomerization to the hydrazone form. As compared to the values in DMSO at 25 °C, the half-lives in water are reduced by a factor of 4033 (35.7 ms) and 1363 (14.6 ms) for **3** and **4**. At physiological temperatures (37 °C) the half-lives are even shorter with 20.9 ms (**3**) and 9.2 ms (**4**) (Table 1). The $t_{1/2}$ values were determined by nanosecond laser flash photolysis (transient spectra at 25 °C and 37 °C for **3** and **4**, see SI Figure S15 and S21).

Table 1. Photostationary states (PSS) and half-lives ($t_{1/2}$) of compounds 1 - 7 measured in DMSO and aqueous media at 25 °C and 37 °C.

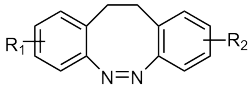

compound	R_1	R_2
1	*m*-OH	*m*-OH
2	*m*-OH	H
3	*p*-OH	*m*-OH
4	*p*-OH	*p*-OH
5	*p*-CH_2OH	*p*-CH_2OH
6	*m*-OH	*p*-CH_2OH
7	*m*-CH_2OH	*m*-CH_2OH

	DMSO			H_2O/D_2O			
compound	PSS $_{Z->E}$[a]	PSS $_{E->Z}$[b]	$t_{1/2}$ (25 °C)[c]	PSS $_{Z->E}$[a]	PSS $_{E->Z}$[b]	$t_{1/2}$ (25 °C)[d]	$t_{1/2}$ (37 °C)[d]
1	43 %	> 99%	12.7 h	36 %	> 99%	42.4 h	9.6 h
2	54 %	> 99%	6.6 h	39 %	> 99%	40.7 h	5.3 h
3	55 %	> 99%	2.4 min	/[e]	> 99%	35.7 ms	20.9 ms
4	29 %	> 99%	19.9 s	/[e]	> 99%	14.6 ms	9.2 ms
5	83 %	> 99%	4.0 h	71 %	> 99%	15.2 h	4.5 h
6	58 %	> 99%	11.2 h	40 %	> 99%	26.1 h	6.1 h
7	81 %	> 99%	11.4 h	64 %	> 99%	31.7 h	5.9 h

[a] irradiation at λ_{max} 385 nm or 405 nm. [b] irradiation at 530 nm. [c] concentration of 200 µM - 1.7 mM. [d] concentration of 200 µM - 420 µM. [e] due to the rapid *E*→*Z* conversion the PSS could not be determined.

Mechanistic studies of the thermal relaxation process

There is general agreement that the thermal back-isomerization of azobenzenes (*Z*→*E*) proceeds via an inversion at one of the N atoms of the azo group.[55] The low preexponential factor (~10^{11} s^{-1}) has been taken as evidence that a non-adiabatic $S_0 \rightarrow T_1 \rightarrow S_0$ spin transition might be involved.[56,57] According to several theoretical studies, the thermal (*E*→*Z*) isomerization of diazocines follows the same mechanism.[28,58–60] Moreover, for diazocines the alternative pathway, rotation around the N=N double bond, is not possible since the azo group is included in a small or medium sized ring.[61,62] In agreement with previous studies on substituted diazocines, the thermal half-lives (*E*→*Z*) of compounds **1**-**2** and **5**-**7** are within the typical range (several hours at room temperature in aprotic organic solvents). Thus, we conclude that the inversion mechanism is operative in these diazocines as well.

As stated above, however, compounds **3** and **4** differ in their UV/Vis spectrum by an additional weak and broad absorption band at ~600 nm and they distinctly deviate in terms of their rapid thermal relaxation rate. Diazocines **3** and **4** (in contrast to **1**-**2** and **5**-**7**) include one or two OH groups in *para* position to the azo group and therefore are susceptible to the azobenzene/phenylhydrazone tautomerism. The analogous 1,7-H shifts are well investigated in *para*-hydroxy azobenzenes.[52,54,63,64] *para*-Hydroxy azobenzene isomerizes (*Z*→*E*) within 200-300 ms in ethanol and has a half-life of 30 min in toluene.[64] *meta*-Hydroxy azobenzene, which cannot tautomerize does not exhibit such a rapid, solvent dependent back-isomerization. Diazocines **3** and **4** with *para*-OH groups behave analogously and isomerize in the millisecond range in water and considerably slower in aprotic solvents (Table 1). We therefore assume a re-isomerization mechanism for the diazocines **3** and **4** in water, similar to the one which has been established for *para*-hydroxy azobenzenes. Figure 5 illustrates the mechanistic steps.

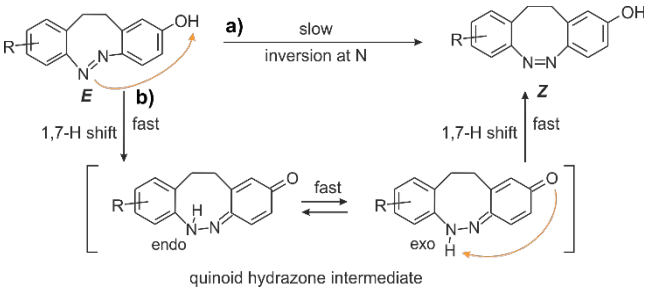

Figure 5. Proposed mechanisms for the thermal relaxation process of dihydroxy diazocines **3** and **4**. Inversion at an azo nitrogen atom (pathway a)) is slow and in water this process is outmatched by the fast mechanism via a phenylhydrazone intermediates (pathway b)). The fast mechanism involves an 1,7-H-shift of the *E* isomer forming the *endo* conformation of the quinoid hydrazone form, followed by a pyramidal inversion at the protonated nitrogen to the *exo* conformation and a 1,7-H-shift to form the *Z* isomer.

Quantum chemical calculations were performed on the mechanism of the thermal *E*-*Z* isomerization of both **3** and **4**. We calculated DLPNO-CCSD(T)/cc-pVTZ(C) single point energies, taking account of solvatization by DMSO using the CPCM method. The geometries were fully optimized at the M06-2X/cc-pVTZ level of theory (for calculated structures of stationary points in the relaxation, see SI Figure S74 and S75). We will now summarize the results for diazocine **3** (Figure 6). The results of calculations on **4** as well as a more detailed description of the results on **3** are provided in the Supporting Information Section 8.1.

To convert *E*-**3** into *Z*-**3**, the reaction has to go via a high-energy transition state TS *E*-**3**/*Z*-**3**. Alternatively, in a protic solvent where a solvent-mediated 1,7-H shift is feasible, the reaction can proceed via s-*E* quinone hydrazone *E*-**3b** and the transition state for the N-H *exo*-*endo* flip (TS *E*-**3b** / *Z*-**3b**) to s-*Z*-quinone hydrazone *Z*-**3b**. The latter would then be converted into *Z*-**3** via another solvent-mediated 1,7-hydrogen shift.

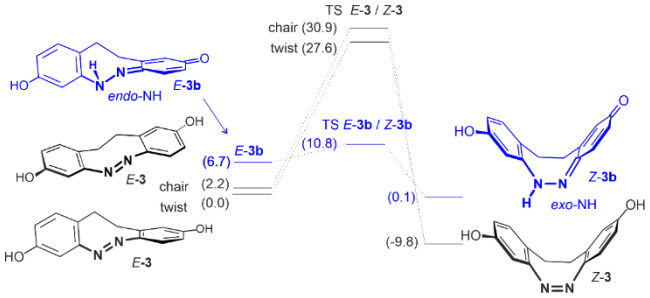

Figure 6. Reaction diagram for conversion of *E*-**3** to *Z*-**3**. Black color coding refers to the high-barrier pathway predicted for aprotic media, blue color coding to the solvent-assisted reaction pathway via the quinone hydrazone tautomers. All electronic energies as calculated at the DLPNO-CCSD(T)/cc-pVTZ (DMSO)//M06-2X/cc-pVTZ level of theory. For more details see Supporting Information Section 8.1

During the 1,7-H shift a hydrogen atom has to be transferred over a distance of about 6 Å from the phenolic OH group to the distant nitrogen atom of the azo group. Three different mechanisms are conceivable for this hydrogen transfer: a) a concerted Grotthuss mechanism through a hydrogen bonded water wire, b) proton transfer via ionic intermediates catalyzed by water molecules and c) hydrogen transfer in H bonded dimers or higher aggregates (Figure 7). Whereas pathways a) and b) include the participation of water, tautomerization via hydrogen bonded dimers or higher aggregates can also be operative in aprotic solvents. This is in agreement with the fact that the relaxation of **3** in DMSO at higher concentrations does not follow a kinetic of first but higher order (for the first and second-order kinetic fit, see SI Figure S22).

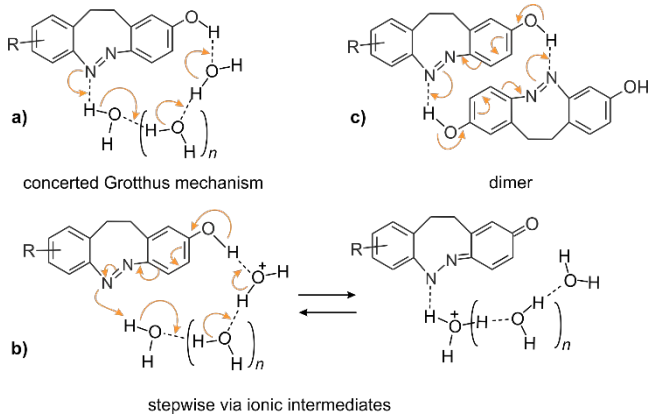

Figure 7. Three conceivable mechanisms for the 1,7-H-shift (azobenzene/phenylhydrazone tautomerization) in dihydroxy diazocines **3** and **4**.

While we were unable to obtain computational evidence for either the concerted Grotthus mechanism (a) or the stepwise ionic mechanism (b), we could optimize stationary points along the reaction coordinate for a tautomerization via dimers (c). According to the results (DLPNO-CCSD(T)), which are described in more detail in the SI, the electronic energy of activation of a concerted twofold hydrogen transfer yielding two equivalents of quinone hydrazone tautomer *E*-**3b** is merely 14.5 kcal mol^{-1}, and thus half the size of the electronic energy of activation for the uncatalyzed reaction. Structures of stationary points along this bimolecular mechanism are shown in Figure S76 (see SI). It is important to note that in this bimolecular mechanism, the quinone hydrazone tautomer s-*E*-**3b** (or s-*E*-**4b**) is formed with an *endo*-NH proton, and that relaxation to the more stable s-*Z*-quinone hydrazones requires an *endo*-*exo* flip of this NH proton. This probably also holds for the water-catalyzed reaction.

To obtain further information about the thermal relaxation mechanism of dihydroxy diazocines **3** and **4** we studied the fast kinetics of the back-isomerization in H_2O and D_2O by nanosecond laser flash-photolysis (Table 2 and 3).

The kinetic isotope effect (KIE) k_H/k_D was determined as 2.43 and 2.78 for diazocines **3** and **4** (transient spectra and eyring plots for **3** and **4**, see SI Figures S56 and S57). This is lower than in most water assisted 1,3-H-shift reactions[65–67] but indicates that H/D transfer is involved in the rate limiting step. The low KIE might be due to the longer water wire in the 1,7-H-shift. A Grotthuss hopping mechanism through several water molecules would also agree with the unusually large negative activation entropy ($\Delta S^{\neq}$) of -107 to -115 J K^{-1} mol^{-1} for the back-isomerization of **3** and **4** in water and D_2O, which indicates a very high degree of order in the transition state. This is in accord with the highly negative activation entropy (-181 J K^{-1}) found for the analogous process in *para*-hydroxy azobenzene in ethanol.[64] The activation enthalpies of 31.3 and 30.9 kJ mol^{-1} are within the range of other water assisted tautomerization reactions.[65–67]

Table 2. Rate constants of the thermal relaxation process measured in aqueous medium (98 % H_2O: 2 % DMSO, k_H) and in D_2O at a concentration of 0.42 mM (k_D) and the kinetic isotope effect (k_H/k_D).

compound	k_H/ s^{-1} 25 °C	k_D/ s^{-1} 25 °C	k_H/k_D 25 °C	k_H/ s^{-1} 37 °C	k_D/ s^{-1} 37 °C	k_H/k_D 37 °C
3	27.0	10.9	2.47	46.8	19.2	2.43
4	64.9	20.7	3.13	105.7	38.0	2.78

Table 3. Activation enthalpies ($\Delta H^{\neq}$) and entropies ($\Delta S^{\neq}$) of dihydroxy diazocines 3 and 4 measured in aqueous medium (H, 0.42 mM) and D_2O (D, 0.42 mM).

compound	$(\Delta H^{\neq})$/ kJ mol^{-1} H	$(\Delta H^{\neq})$/ kJ mol^{-1} D	$(\Delta S^{\neq})$/ J K^{-1} mol^{-1} H	$(\Delta S^{\neq})$/ J K^{-1} mol^{-1} D
3	31.3	32.7	-113	-115
4	30.9	33.0	-107	-109

Summing up, we state that the diazocines lacking *para*-OH groups (**1**, **2**, **5**-**7**) re-isomerize via the conventional nitrogen inversion process (path a) in Figure 5). The diazocines with *para*-OH groups (**3**, **4**) follow the tautomerization pathway (b) in Figure 5). In aprotic solvents the 1,7-H-shift is mediated by aggregation (Figure 7c)) and in water either a concerted Grotthuss mechanism or proton hopping via ionic intermediates is operative (Figure 7a) and b)). We cannot distinguish between the latter two mechanisms however, the highly negative activation entropy is indicative for a concerted mechanism via a water wire.[67]

Kinetics of the relaxation process in the presence of cyclodextrins

The proposed 1,7-H shift mechanisms shown in Figure 7 have a considerable larger activation volume than the conventional inversion mechanism. The water assisted mechanisms (Figure 7a) and b)) require at least three water molecules included in the transition state, and the aggregation pathway c) demands at least double the activation volume as compared to the unimolecular inversion mechanism. Hence, inclusion of the diazocines in a hydrophobic cavity of a suitable size should impede the fast tautomerization processes and leave the slow inversion as the only remaining isomerization pathway. Cyclodextrins (CDs) are water soluble host compounds with hydrophobic cavities, and they are available in different sizes. The three commercially available CDs: α-, β- and γ cyclodextrin have inner diameters of 4.7–5.3 Å, 6.0–6.5 Å, and 7.5–8.3 Å.[68–70] Simple model calculations at the ωB97X-D3/def2-SVP level of theory (xtb, ORCA 5.0.1, see SI Section 8.2 for more detail)[71–78] of dihydroxy diazocine **3** reveal that α-CD is too small, β-CD fits well and γ-CD leaves remaining space after inclusion of the diazocines (Figure 8). For detailed molecular dynamics (MD) simulations including explicit water see SI figure 80-88. The MD calculations as well indicate that diazocine **3** is tightly bound inside β-CD and that no water molecules are able to enter the cavity. Thus, the fast back-isomerization via tautomerization is inhibited.

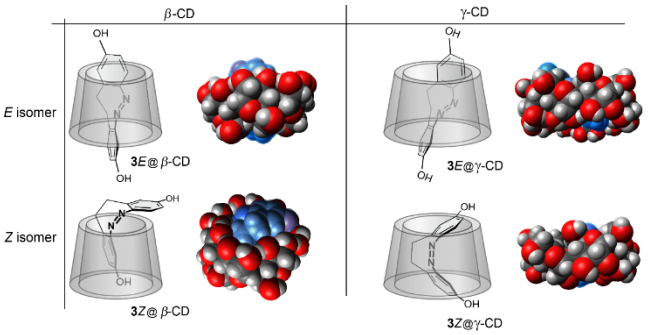

Figure 8. Model calculations of diazocine **3** in *E* and *Z* configuration inside the cavity of β- and γ-cyclodextrin (ωB97X-D3/def2-SVP). The structures are shown with van der Waals radii of C, H, N, and O atoms. The diazocines are colored in blue. For a better illustration of the binding modes, the structures are also given as schematic representations. No inclusion structure was found for α-cyclodextrin because of severe van der Waals clashes between the diazocine and α-CD inside the cavity, which is obviously too small to accommodate the diazocine. For more details see SI Section 8.2.

It is interesting to note that β-CD binds the slender *E* isomer tightly, however, does not include the bent *Z* isomer. Only one of the phenyl rings intrudes the cavity. The azo group remains exposed to the solvent, whereas the larger γ-CD completely encloses both the *E* and the *Z* isomer.

Experiments were performed to investigate the influence of α-, β- and γ-CD on the kinetics of the reisomerization of diazocines **3** and **4** in water. Because of the limited solubility particularly of β-CD in water we employed the corresponding 2-hydroxypropyl substituted CDs. The kinetics were measured by laser flash photolysis (for transient spectra of **3** and **4** in presence of CDs, see SI Figure S30 and S31). Table 4 summarizes the results. As a reference compound, which cannot undergo tautomerization, dihydroxy diazocine **1** is included. For compound **1** the half-lives ($t_{½}$) in presence of CDs were determined by UV/Vis absorption spectroscopy (for UV/Vis spectra of **1** in presence of CDs, see SI Figure S26-S29).

Table 4. Half-lives ($t_{1/2}$) of the *E* isomers of phenol-type diazocines 1, 3 and 4 (185 µM) at 37°C in different environments. CD =(2-hydroxypropyl)-cyclodextrin (278 mM, 1500-fold excess).

environment	1	3	4
H_2O	10.8 h	26 ms	12 ms
H_2O/ α-CD	8.6 h	1.8 ms	0.3 ms
H_2O/ β-CD	4.0 h	274 ms	159 ms
H_2O/ γ-CD	6.6 h	92 ms	54 ms

Addition of an excess of cyclodextrins to the reference compound **1** accelerates the back-isomerization, however, the half-life of the *E* isomer stays within the range of hours. The situation is different in case of **3** and **4**. Addition of α-CD to the aqueous solution of **3** and **4** accelerates the reisomerization by a factor of 14 (1.8 ms) and 40 (0.3 ms). A reverse effect is observed upon addition of β-CD. The reaction is slowed down by a factor of 10.5 (274 ms) for **3** and 13.3 (159 ms) for **4**. γ-CD decelerates the back-reaction less efficiently than β-CD. Hence, the addition of β-CD has the same effect on the half-lives of the *E* isomers of diazocines **1** (decrease), **3** and **4** (increase), as changing the solvent from water to unpolar organic solvents (for UV/Vis spectra of **1**, **3** and **4** in diethyl ether, see SI Figure S23-S25).

The slower reaction in the presence of β-CD is expected. The diazocines are tightly bound inside the hydrophobic cavity (Figure 7) hence, the azophenol unit is shielded from water preventing the fast tautomerization process (Figure 6, 7). Conversion to the phenylhydrazone tautomer via dimers or higher aggregates is prevented by a lack of space inside the cavity. Reisomerization can only proceed by the conventional slow inversion process or after leaving the cavity in a fast equilibrium between free and bound diazocine. γ-CD is less effective in slowing down the reaction rate because there might be sufficient space inside the cavity to accommodate additional water molecules or by a weaker binding and higher concentrations of the free diazocines. We have no sound explanation for the acceleration by α-CD. One might speculate that the diazocines bind outside the cavity and the existing, preformed $\cdots(OH)_n\cdots OH\cdots$ wire at the brim of α-CD bridges the azo N and the phenol O atom favoring the Grotthuss mechanism or proton hopping that would otherwise proceed through a dynamic water wire in bulk water.

Besides the re-isomerization kinetics, the photostationary state ($PSS_{Z\rightarrow E}$) is affected in the presence of *β*-CD. Upon addition of *β*-CD to a solution of diazocine **1** and irradiation with 385 nm the $PSS_{Z\rightarrow E}$ increases from 36% asymptotically to 50% at a 20fold excess of *β*-CD (for the plot of Fraction of *E*-**1** in the PSS depending on the concentration of CD see SI Figure S89). The natural estrogen receptor is more efficient in stabilizing the Z isomer of **1** and therefore might increase the PSS even well above 50%.

In summary, aprotic solvents as well as the inclusion of diazocines **3** and **4** in the tight hydrophobic cavity of β-cyclodextrin substantially extend the lifetime of the metastable *E* isomers. DFT and MD calculations reveal that this is due to the inhibition of fast tautomerization process, which limits the lifetime in solution.

Biological Testing – Reporter Gene Assay

To measure estrogenic activity of *E* and *Z* configurations of the diazocine compounds, a cell-based reporter gene assay has been established, analogous to methods published previously.[79–83] Shortly, estrogen receptor (ER)-positive MCF-7 breast cancer cells were used and transfected with plasmids containing the gene sequence for firefly luciferase under the control of the estrogen response element (ERE). If an ER ligand exhibits estrogenic activity, ERE is activated and leads to the expression of firefly luciferase. As readout, the luminescence generated in the luciferase-catalyzed reaction was measured. This luminescence signal is proportional to the estrogenic activity of the ligand compound. First, the reporter gene assay was established for the reference β-estradiol. Herein, the incubation time of the estrogen with the transfected cells could be minimized to 15 h. The EC_{50} value determined for *β*-estradiol in our assay (13.4 ± 1.7 pM) is in good agreement with the data reported in the literature (15 ± 2 pM).[84] For exemplary dose-response curve see SI Figure S58. In addition, we applied *para*-hydroxy azobenzenes as further controls under light controlled conditions. For these compounds, a strong estrogenic activity could be verified in the cellular reporter gene assay (for dose-response curve see SI Figure S59), which is in line with the literature.[24,85] Furthermore, irradiation tolerance of the cell assay was verified by dose-response analysis of reference β-estradiol with and without irradiation (for dose-response curve see SI Figures S61-S64). Every assay includes β-estradiol as a reference for the maximum estrogenic activity, since expression of ER varies from cell passage to cell passage.

Having our assay validated to provide meaningful results, dose-response analysis of the diazocine based photoswitchable estrogen receptor modulators was performed in a darkened laboratory under red light to avoid uncontrolled isomerization. Each compound was tested not-irradiated (dark, *Z* isomer) as well as irradiated (PSS 405 nm or 385 nm). For PSS testing, the compounds were first irradiated in DMSO before addition to the cells (1% final DMSO concentration, see SI Section 6 for experimental details), due to a better PSS in DMSO compared to the aqueous medium. Based on the short half-lives of the *E* diazocines at 37 °C, only one-time irradiation at the beginning of the 15 h total incubation time was not sufficient to detect an estrogenic effect in the cell assay (for dose-response curve see SI Figure S60). Consequently, the cell assay was irradiated for 60 s (405 nm) or 180 s (385 nm with reduced intensity see SI Section 7 for additional experimental details) every 3 h during the 15-hours-long incubation time. For this purpose, a custom-made lamp for the cell incubator was used, which could be programmed by a timer (for lamp specification see SI Section 7). Prior to the cell experiments, intensity, and duration of the irradiation necessary to reach the PSS of the diazocines was determined by UV-spectroscopy under similar but cell free conditions (for UV/ Vis spectra see SI Figures S71-S73). Maximum relative activities (max. rel. act.) referring to maximum activity of β-estradiol are given for all test compounds with and without irradiation in Table 5.

meta-Substituted diazocines **1** and **2** (Figure 9) show an approx. 3-fold increase in their estrogenic activity upon exposure to 405 nm light according to the above irradiation scheme (blue squares, max. rel. act.: 68 ± 11 % (**1**) and 114 ± 18 % (**2**), respectively). Non-irradiated compounds exhibit only slight estrogenic activities at the highest concentrations (red circles,

max. rel. act.: 27 ± 3 % (**1**) and 39 ± 6 % (**2**), respectively). Irradiated disubstituted diazocine **1** shows a much improved EC_{50} value (4.7 ± 1.2 µM) compared to monosubstituted diazocine **2** (EC_{50} = 38.0 ± 13.1 µM). In comparison to the highly potent β-estradiol (EC_{50} = 13.4 ± 1.7 pM), the diazocines seem to be weak estrogen receptor agonists. However, considering the fact that the PSS in aqueous solution is only 28 % (*E*-**1**) or 39 % (*E*-**2**) providing only a minor portion of the bioactive isomer, the *E* diazocines can be considered as quite potent.

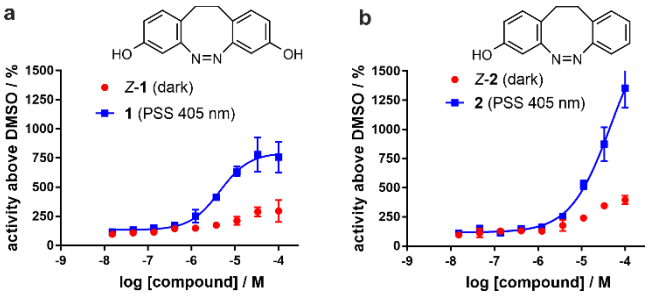

Figure 9. Estrogenic activities of *meta*-substituted diazocines **1** and **2** in a cell-based reporter gene assay. a) Disubstituted diazocine **1**, unirradiated (dark, red circles) vs. irradiated at 405 nm for 60 s every 3 h (PSS 405 nm, blue squares, EC_{50} = 4.7 ± 1.2 µM). b) Monosubstituted diazocine **2**, unirradiated (dark, red circles) vs. irradiated at 405 nm for 60 s every 3 h (PSS 405 nm, blue squares, EC_{50} = 38.0 ± 13.1 µM). The dose-response curves show one representative example from at least three independent cell assays. Data points are means of technical triplicates ± SD. EC_{50}-values are means of biological replicates ± SD.

Surprisingly, the unsymmetrical diazocine **3** also shows a moderate estrogenic activity in the same assay (60 s irradiation time, applied five times every 3 h, Figure 9 a, max. rel. act.: 52 ± 5 %, EC_{50} cannot be determined reliably). Despite the extremely short half-life of the bioactive *E* isomer in the millisecond range (20.9 ms in water at 37 °C), an unexpected distinct estrogenic activity was observed. More frequent irradiation of diazocine **3** every 30 min (instead of every 3 h), did not lead to an increase in activity (for dose-response curve see SI Figure S65 a). Obviously, the estrogenic activity of the *in situ* photogenerated *E* isomer (> 3 h) exceeds its half-lifetime (20.9 ms) by a factor of at least 500 000. In contrast, *para*-disubstituted diazocine **4** did not exhibit significant estrogenic activity, neither after irradiation every 3 h (Figure 10 b) nor after irradiation every 30 min (for dose-response curve see SI Figure S65 b). As a possible explanation, the half-life of the *E* isomer (9.2 ms in water at 37 °C) is too short for effective initial binding to the receptor. Additionally, no mechanism extending the lifetime of the bioactive *E* isomer is present to generate a measurable estrogenic activity above the background activity of the *Z* isomer.

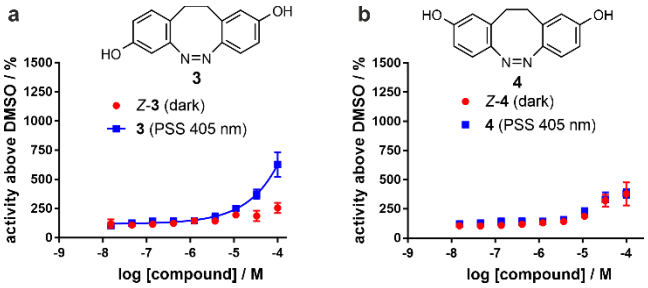

Figure 10. Estrogenic activities of *para*-substituted diazocines **3** and **4** in a cell-based reporter gene assay. a) Unsymmetrical diazocine **3**, unirradiated (dark, red circles) vs. irradiated at 405 nm for 60 s every 3 h (PSS 405 nm, blue squares, EC_{50} cannot be determined reliably). b) *para*-Disubstituted diazocine **4**, unirradiated (dark, red circles) vs. irradiated at 405 nm for 60 s every 3 h (PSS 405 nm, blue squares). Dose-response curves are each one representative example from at least three independent cell assays. Data points are means of technical triplicates ± SD.

Based on the tautomerization hypothesis of *para*-OH-diazocines, we synthesized compounds **5-7** with benzylic alcohol units. As expected, no evidence for the tautomerization process could be found and the compounds showed half-lives of several hours with high PSSs values (58-83% *E* isomer). Diazocines **5-7** were tested analogous to diazocines **1-4** in the reporter gene assay (for dose-response curve see SI Figure S66). Herein, **5** and **7** exhibit no measurable estrogenic activity. Compound **6** with one phenolic OH group in *meta*-position and one benzylic OH group in *para*-position shows limited estrogenic activity. Obviously, at least one phenol type OH group is needed to trigger estrogenic activity of hydroxy diazocines. Table 5 summarizes the maximum relative activities of diazocines **1-7** before and after irradiation.

Table 5. Overview of maximum relative activities hydroxy-functionalized diazocines 1-7 referring to maximum activity of β-estradiol in the respective estrogen reporter assay. Each compound was tested unirradiated (dark, *Z*-isomer) as well as irradiated every 3 h (PSS 405 nm or 385 nm). Data are means ± SD. Each compound was tested in technical triplicates in at least three independent biological replicates.

#	max. relative activity *Z* isomer (dark)	max. relative activity PSS 405 nm/ 385 nm
1	27 ± 3 %	68 ± 11 %
2	39 ± 6 %	114 ± 18 %
3	21 ± 3 %	52 ± 5 %
4	46 ± 16 %	45 ± 18 %
5	24 ± 4 %	45 ± 9 %
6	33 ± 4 %	81 ± 1 %
7	16 ± 5 %	20 ± 11 %

Compounds **4** and **5** that did not show an estrogenic effect in the reporter gene assay, were investigated with respect to a potential antagonist effect. Thus, the diazocines were incubated together with the agonist β-estradiol in the reporter gene assay to check if they are able to reduce the estrogenic activity. As a positive control for an antagonistic effect, raloxifene was used

(for dose-response curve see SI Figure S67). For both diazocines **4** and **5** no antagonistic effect could be observed, neither for the unirradiated *Z*-isomers nor after irradiation every 3 h (for dose-response curve see SI Figure S68).

In conclusion we state that diazocines **1** and **2** are efficient photoswitchable estrogens, which have 27% (**1**) and 39% (**2**) of the maximum relative activity of estradiol in the *Z* (dark) state and 68% (**1**) and 114% (**2**) after irradiation to the photostationary states (**1** *E*: 28%, **2** *E*: 39%). Half-lifes of the bioactive *E* state at 37°C are 9.6 h (**1**) and 5.3 h (**2**), respectively. Very surprisingly, diazocine **3** is also estrogen active after irradiation with 405 nm, despite the half-life of the biologically active *E* isomer in water being in the millisecond range. These results further suggest a significant inhibition of the fast tautomerization process leading to a longer half-life, when the ligand is bound to its receptor.

Active back-switching by irradiation at 525 nm

In more detail, there are three conceivable hypotheses that would explain why the *E* isomer of diazocine 3 is more than 500 000 times longer active in the reporter gene assay compared to its very short lifetime in water.

1. The transcription process in the reporter gene assay continues for more than 3 h, once triggered by short-lived *E*-**3**

2. *E*-**3** is thermodynamically stabilized by strong binding in the estrogen receptor and its lifetime thus is extended

3. *E*-**3** is kinetically stabilized by inhibition of the tautomerization process inside the hydrophobic cavity of the estrogen receptor in a similar fashion as shown by the experiment with β-cyclodextrin.

Notably, studies with ligands and the isolated estrogen receptor protein were not feasible due to interference between the readout of commercially available fluorescence-based binding assays and the absorption range of the diazocines that would lead to back-switching and subsequent inactivation of the diazocines. Hence, to check hypothesis 1, we performed the following experiment. As in the previous assay settings, we irradiated the cell assay in the presence of diazocines **1**, **2**, **3** and **6**, which showed significant estrogenic activities in the *E* state, with 405 nm or 385 nm and repeated this irradiation every 3 h over a total period of 15 h. However, in contrast to the previous irradiation scheme, 10 minutes after every irradiation, exposure to 525 nm (green) light for 20 s was applied (irradiation protocol for compounds **1-3** see Figure 11 a). Green light is very efficient in enforcing back-isomerization of all diazocines (PSS > 99% *Z* isomer, Table 1). It can be safely assumed that even a stabilized complex of the estrogen receptor with the *E* isomer of the diazocine would be decomposed during the 20 s exposure time to 525 nm light. Figure 10 presents the results of these experiments for diazocines **1-3**. For for dose-response curve of compound **6** see SI Figure S69.

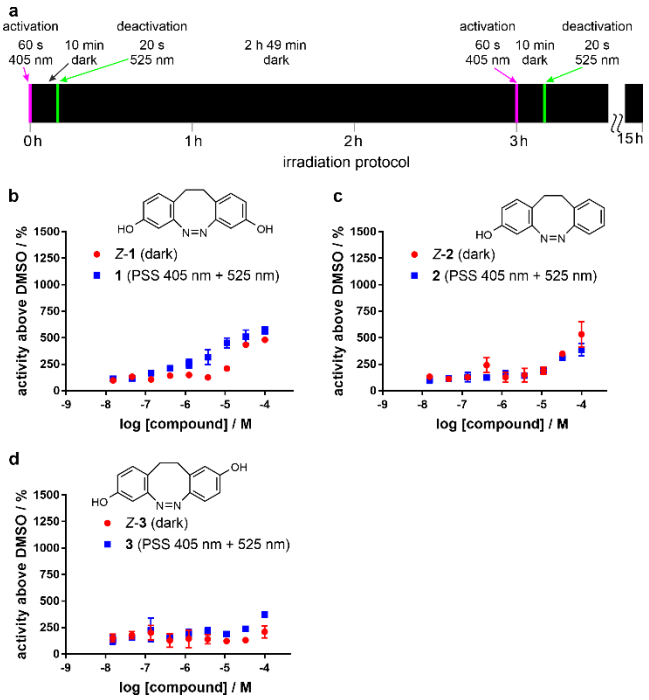

Figure 11. Estrogenic activities of **1**, **2** and **3** after an irradiation scheme including photochemically enforced back-isomerization with 525 nm (green light) a) Irradiation protocol: *Z*→*E* isomerization (activation) is induced by a 60 s period of irradiation with 405 nm. After 10 min in the dark, the cell-based reporter assay is irradiated with 525 nm light, which leads to complete back-isomerization of the diazocines to the biologically inactive *Z* isomers. After almost 3 h this irradiation sequence is repeated 4 times. The total incubation time was 15 h. b-d) Dose response points corresponding to samples that are left in the dark, are indicated with red circles. Blue squares represent data obtained after applying the irradiation scheme including exposure to 525 nm light. Dose-response curves are one representative example from two independent cell assays. Data points are means of technical triplicates ± SD.

None of the diazocines **1**, **2**, **3** and **6**, which showed significant estrogenic activity in the previous reporter assay, exhibited a measurable switchable estrogenic activity in this experiment using green light. The formerly bioactive isomers almost reproduce the dose-response curves of the unirradiated compounds. This is expected if one assumes that the generally accepted signal transduction cascade (estrogen binding → receptor dimerization → translocation → DNA binding → co-activator recruitment → transcription process) is interrupted as soon as estradiol, or a photoswitchable estrogen-active compound, leaves the receptor. The active *E* isomers of compounds **1**, **2** and **6** show half-lives of more than 5 h. Hence, thermal relaxation in our previous experiments left sufficient concentrations of the active isomer until the next irradiation was applied after 3h. The concentration of the active *E* isomer that was maintained during the whole incubation time of 15 h was sufficient to sustain the transcription process and to measure estrogenic activity in the cell assay. In contrast, deactivation with green light (525 nm) 10 minutes after photoactivation, however, obviously interrupts the signal transduction pathway. Significantly, the 10 minutes presence of active *E* isomers is not sufficient to sustain the tran-

scription process. Again, the behaviour of diazocine **3** is remarkable. The half-life of the *E*-**3** isomer in pure water is only 20.9 ms (Table 1). Hence, 10 minutes (28 000 half-lives) after activation with 405 nm, no active *E* isomer should be left in solution. Nevertheless, when *E*-**3** is incubated in the estrogen reporter gene assay, transcription continues for at least 3 h after photoactivation (first experiment, Figure 10 a), unless the biological activity is switched off by irradiation with 525 nm (second experiment, Figure 11 d)

Discussion

The results summarized in Figure 11 provide strong evidence that hypothesis 1 (transcription process in the reporter gene assay, once triggered by short-lived *E*-**3** continues for more than 3 h) can be rejected. Otherwise, estrogenic activity couldn't be shut off by back-isomerization of *E*-**3** with green light. Hypothesis 2 (thermodynamic stabilization of *E*-**3**), and hypothesis 3 (kinetic stabilization of *E*-**3**) are left as viable explanations for the extended estrogenic activity of *E*-**3**. It is indeed known that high energy conformations of small molecules can be stabilized by binding to protein receptors.[86–88] A similar modulation could well apply to the high energy isomer *E*-**3** when bound to the estrogen receptor. An extensive study of ligands and ligand-protein complexes revealed that the overall stabilization energies do not exceed 3 kcal mol^{-1}.[86] This is sufficient to stabilize conformations that are not detectable by NMR in equilibrium in water, however, cannot fully account for the 9.8 kcal mol^{-1} energy difference of *Z*-**3** and *E*-**3**. We consider the kinetic stabilization of *E*-**3** inside the estrogen receptor blocking the key tautomerization process as the major factor for its extended lifetime in the cell assay. The strong solvent dependence of the half-live (35.7 ms in water, 2.4 min in DMSO and 8 min in diethyl ether at 25°C (see UV/ Vis spectra SI Figure S24)) indicates that the compound´s environment has a crucial influence on its lifetime. In line with this notion, stabilization of *E*-**3** occurs in the hydrophobic cavity of β-cyclodextrin (Figure 8, Table 4). Upon addition of β-cyclodextrin to an aqueous solution of **3** the half-life of *E*-**3** is extended by a factor of >10. Estradiol and, according to our molecular modelling studies also *E*-**3**, are tightly bound in the hydrophobic cavity of the estrogen receptor. The cavity is surrounded by lipophilic amino acids such as several leucine residues, alanine, phenylalanine and methionine. At both ends of the active site, the more polar residues arginine, glutamine and histidine form hydrogen bonds with the OH groups of the estrogenic ligand. Since there is no space left for water to be included inside the cavity, the fast back-isomerization of *E*-**3** via the tautomerization mechanism is prohibited. The alternative fast isomerization mechanism via dimerization is impeded as well by a lack of space. Thus, we conclude that thermodynamic stabilization and more importantly kinetic stabilization by shutting down the fast back-isomerization processes accounts for the extended lifetime of the active state and subsequent measured estrogenic activity of the diazocine compound **3**.

Conclusion

According to molecular modeling studies, several dihydroxy-substituted diazocines in their metastable *E* configuration exhibit remarkable structural similarities with estradiol and similar binding modes in the estrogen α receptor. The corresponding stable *Z* isomers are predicted not to bind inside the active site cavity of the receptor. These theoretical studies suggested that dihydroxy diazocines could be potentially used as photoswitchable estrogens.

Seven (di)hydroxy diazocines were synthesized and their photophysical properties were determined. They exhibit similar photoswitching properties in aprotic, organic solvents. In water, two (**3** and **4**) of the seven diazocines with *para* OH groups exhibit *E* isomers with thermal half-lives in the millisecond range, whereas the lifetimes of the other substituted diazocines remain in the range of hours. Kinetic data and kinetic isotope effects reveal that 1,7-H-shifts via the tautomeric hydrazine intermediates are responsible for the ultrafast solvent-dependent back-isomerization of *p*-OH-diazocines. Addition of β-cyclodextrin to the aqueous solution of *p*-OH-diazocines **3** and **4** leads to a deceleration of the back-isomerization of the *E* isomers by a factor of >10. Model calculations indicate that the *E* isomers are included in the hydrophobic cavity of β-cyclodextrin thus preventing the fast tautomeric $E \rightarrow Z$ back-reaction.

Biological studies in a reporter gene assay show photoswitchable estrogenic activities for compounds **1**, **2**, **3** and **6**. Particularly diazocine **1** and **2** are very efficient in this regard, with 39% of the maximum relative activity of estradiol in the *Z* (dark) state and 114% after irradiation in the photostationary state (46% *Z*/54% *E*). Very surprisingly, diazocine **3** is also estrogenically active after irradiation with 405 nm, even though the half-life of the biologically active *E* isomer in water is in the millisecond range. Our experiments strongly indicate that the lifetime of the *E* isomer is extended by a factor of > 500 000 when bound within the estrogen receptor. We assume that the mechanism is similar to the β-cyclodextrin effect: the hydrophobic cavity in the binding pocket of the estrogen receptor prevents the fast tautomeric re-isomerization and it stabilizes the metastable *E* isomer thermodynamically by strong binding. Photoswitchable drugs with short lifetimes of their active state in water but biologically active for an extended period of time in biological environments have been reported before.[89–91] Similar stabilization mechanisms might be operative in these cases.

Our results suggest such photoswitchable drugs are only active if both the receptor is present and light is applied to the same spot. This could greatly increase the spatial resolution of photopharmacological applications. In case of diazocine **3** the active state would be inactivated with a half-life of 20.9 ms after leaving the receptor. This translates to a diffusion pathlength of <5μm. Hence, the drug activity could be restricted to an area that is in the size range of typical components of a cell, which should allow detailed biological investigations. Diazocine **2** probably is a good starting point for the development of photoswitchable estrogen receptor agonists and antagonists for the targeted treatment of breast cancer and other hormone dependent cancers.

ASSOCIATED CONTENT

Supporting Information.

The Supporting Information (analytical equipment, molecular modeling, syntheses, photochemical characterization, kinetic studies, biological evaluation, computational details) is available free of charge via the Internet at http://pubs.acs.org."

AUTHOR INFORMATION

Corresponding Author

* E-mail: rherges@oc.uni-kiel.de (R.H.);
cpeifer@pharmazie.uni-kiel.de (C.P.)

Author Contributions

All authors have given approval to the final version of the manuscript.
‡These authors contributed equally.

Funding Sources

We are grateful for support by the Deutsche Bundesstiftung Umwelt (DBU) and the Deutsche Forschungsgemeinschaft via SFB 677.

Notes

Any additional relevant notes should be placed here.

ACKNOWLEDGMENT

The authors thank Georg Gescheidt-Demmer and Dmytro Neshchadin (University of Graz) for NMR binding studies. The authors are grateful to Dr. Claus Bier for building the cell incubator lamp. Furthermore, the authors would like to thank the Tholey working group for the native MS measurements.

ABBREVIATIONS

ERα, estrogen receptor α; ERβ, estrogen receptor β; PSS, photostationary states

REFERENCES

(1) Hopkins, A. L. Network pharmacology: the next paradigm in drug discovery. *Nat. Chem. Biol.* **2008**, *4* (11), 682–690.

(2) Velema, W. A.; Szymanski, W.; Feringa, B. L. Photopharmacology: beyond proof of principle. *J. Am. Chem. Soc.* **2014**, *136* (6), 2178–2191.

(3) Lerch, M. M.; Hansen, M. J.; van Dam, G. M.; Szymanski, W.; Feringa, B. L. Emerging Targets in Photopharmacology. *Angew. Chem. Int. Ed.* **2016**, *55* (37), 10978–10999.

(4) Szymański, W.; Beierle, J. M.; Kistemaker, H. A. V.; Velema, W. A.; Feringa, B. L. Reversible photocontrol of biological systems by the incorporation of molecular photoswitches. *Chem. Rev.* **2013**, *113* (8), 6114–6178.

(5) Hüll, K.; Morstein, J.; Trauner, D. In Vivo Photopharmacology. *Chem. Rev.* **2018**, *118* (21), 10710–10747.

(6) Brieke, C.; Rohrbach, F.; Gottschalk, A.; Mayer, G.; Heckel, A. Light-controlled tools. *Angew. Chem. Int. Ed.* **2012**, *51* (34), 8446–8476.

(7) Hoorens, M. W. H.; Szymanski, W. Reversible, Spatial and Temporal Control over Protein Activity Using Light. *Trends Biochem. Sci* **2018**, *43* (8), 567–575.

(8) Broichhagen, J.; Frank, J. A.; Trauner, D. A roadmap to success in photopharmacology. *Acc. Chem. Res.* **2015**, *48* (7), 1947–1960.

(9) Trads, J.; Hüll, K.; Matsuura, B.; Laprell, L.; Fehrentz, T.; Görldt, N.; Kozek, K. A.; Weaver, D.; Klöcker, N.; Barber, D.; Trauner, D. Sign Inversion in Photopharmacology: Incorporation of Cyclic Azobenzenes in Photoswitchable Potassium Channel Blockers and Openers. *Angew. Chem. Int. Ed.* **2019**, *58*, 15421-15428.

(10) Fuchter, M. J. On the Promise of Photopharmacology Using Photoswitches: A Medicinal Chemist's Perspective. *J. Med. Chem.* **2020**, *63* (20), 11436–11447.

(11) Welleman, I. M.; Hoorens, M. W. H.; Feringa, B. L.; Boersma, H. H.; Szymański, W. Photoresponsive molecular tools for emerging applications of light in medicine. *Chem. Sci.* **2020**, *11* (43), 11672–11691.

(12) Diamanti-Kandarakis, E.; Bourguignon, J.-P.; Giudice, L. C.; Hauser, R.; Prins, G. S.; Soto, A. M.; Zoeller, R. T.; Gore, A. C. Endocrine-disrupting chemicals: an Endocrine Society scientific statement. *Endocr. Rev.* **2009**, *30* (4), 293–342.

(13) Robledo, C.; Peck, J. D.; Stoner, J. A.; Carabin, H.; Cowan, L.; Koch, H. M.; Goodman, J. R. Is bisphenol-A exposure during pregnancy associated with blood glucose levels or diagnosis of gestational diabetes? *J. Toxicol. Environ. Health - A* **2013**, *76* (14), 865–873.

(14) Beek, T. aus der; Weber, F.-A.; Bergmann, A.; Hickmann, S.; Ebert, I.; Hein, A.; Küster, A. Pharmaceuticals in the environment—Global occurrences and perspectives. *Environ. Toxicol. Chem.* **2016**, *35* (4), 823–835.

(15) Yoon, K.; Kwack, S. J.; Kim, H. S.; Lee, B.-M. Estrogenic endocrine-disrupting chemicals: molecular mechanisms of actions on putative human diseases. *J. Toxicol. Environ. Health - B* **2014**, *17* (3), 127–174.

(16) Dahlman-Wright, K.; Cavailles, V.; Fuqua, S. A.; Jordan, V. C.; Katzenellenbogen, J. A.; Korach, K. S.; Maggi, A.; Muramatsu, M.; Parker, M. G.; Gustafsson, J.-A. International Union of Pharmacology. LXIV. Estrogen receptors. *Pharmacol. Rev.* **2006**, *58* (4), 773–781.

(17) Klinge, C. M. Estrogen receptor interaction with estrogen response elements. *Nucleic Acids Res.* **2001**, *29* (14), 2905–2919.

(18) Hall, J. M.; Couse, J. F.; Korach, K. S. The multifaceted mechanisms of estradiol and estrogen receptor signaling. *J. Biol. Chem.* **2001**, *276* (40), 36869–36872.

(19) Yaşar, P.; Ayaz, G.; User, S. D.; Güpür, G.; Muyan, M. Molecular mechanism of estrogen-estrogen receptor signaling. *Reprod. Med. Biol.* **2017**, *16* (1), 4–20.

(20) Bafna, D.; Ban, F.; Rennie, P. S.; Singh, K.; Cherkasov, A. Computer-Aided Ligand Discovery for Estrogen Receptor Alpha. *Int. J. Mol. Sci.* **2020**, *21* (12), 4193, 1-60.

(21) Shao, W.; Brown, M. Advances in estrogen receptor biology: prospects for improvements in targeted breast cancer therapy. *Breast Cancer Res.* **2004**, *6* (1), 39–52.

(22) Mitlak, B. H.; Cohen, F. J. Selective estrogen receptor modulators: a look ahead. *Drugs* **1999**, *57* (5), 653–663.

(23) Riggs, B. L.; Hartmann, L. C. Selective estrogen-receptor modulators—mechanisms of action and application to clinical practice. *New Engl. J. Med.* **2003**, *348* (7), 618–629.

(24) Sanoh, S.; Kitamura, S.; Sugihara, K.; Fujimoto, N.; Ohta, S. Estrogenic Activity of Stilbene Derivatives. *J. Health Sci.* **2003**, *49* (5), 359–367.

(25) Pianowski, Z. L. Recent Implementations of Molecular Photoswitches into Smart Materials and Biological Systems. *Chemistry* **2019**, *25* (20), 5128–5144.

(26) Morstein, J.; Trads, J. B.; Hinnah, K.; Willems, S.; Barber, D. M.; Trauner, M.; Merk, D.; Trauner, D. Optical control of the nuclear bile acid receptor FXR with a photohormone. *Chem. Sci.* **2020**, *11* (2), 429–434.

(27) Willems, S.; Morstein, J.; Hinnah, K.; Trauner, D.; Merk, D. A Photohormone for Light-Dependent Control of PPARα in Live Cells. *J. Med. Chem.* **2021**, *64* (14), 10393–10402.

(28) Lentes, P.; Stadler, E.; Röhricht, F.; Brahms, A.; Gröbner, J.; Sönnichsen, F. D.; Gescheidt, G.; Herges, R. Nitrogen Bridged Diazocines: Photochromes Switching within the Near-Infrared Region with High Quantum Yields in Organic Solvents and in Water. *J. Am. Chem. Soc.* **2019**, *141* (34), 13592–13600.

(29) Moormann, W.; Tellkamp, T.; Stadler, E.; Röhricht, F.; Näther, C.; Puttreddy, R.; Rissanen, K.; Gescheidt, G.; Herges, R. Efficient

Conversion of Light to Chemical Energy: Directional, Chiral Photoswitches with Very High Quantum Yields. *Angew. Chem. Int. Ed.* **2020**, *59*, 15081-15086.

(30) Siewertsen, R.; Neumann, H.; Buchheim-Stehn, B.; Herges, R.; Näther, C.; Renth, F.; Temps, F. Highly efficient reversible Z-E photoisomerization of a bridged azobenzene with visible light through resolved S(1)(n pi*) absorption bands. *J. Am. Chem. Soc.* **2009**, *131* (43), 15594–15595.

(31) Hammerich, M.; Schütt, C.; Stähler, C.; Lentes, P.; Röhricht, F.; Höppner, R.; Herges, R. Heterodiazocines: Synthesis and Photochromic Properties, Trans to Cis Switching within the Bio-optical Window. *J. Am. Chem. Soc.* **2016**, *138* (40), 13111–13114.

(32) Albert, L.; Peñalver, A.; Djokovic, N.; Werel, L.; Hoffarth, M.; Ruzic, D.; Xu, J.; Essen, L.-O.; Nikolic, K.; Dou, Y.; Vázquez, O. Modulating Protein-Protein Interactions with Visible-Light-Responsive Peptide Backbone Photoswitches. *ChemBioChem* **2019**, *20* (11), 1417–1429.

(33) Cabré, G.; Garrido-Charles, A.; González-Lafont, À.; Moormann, W.; Langbehn, D.; Egea, D.; Lluch, J. M.; Herges, R.; Alibés, R.; Busqué, F.; Gorostiza, P.; Hernando, J. Synthetic Photoswitchable Neurotransmitters Based on Bridged Azobenzenes. *Org. Lett.* **2019**, *21* (10), 3780–3784.

(34) Glock, P.; Broichhagen, J.; Kretschmer, S.; Blumhardt, P.; Mücksch, J.; Trauner, D.; Schwille, P. Optical Control of a Biological Reaction-Diffusion System. *Angew. Chem. Int. Ed.* **2018**, *57* (9), 2362–2366.

(35) Heintze, L.; Schmidt, D.; Rodat, T.; Witt, L.; Ewert, J.; Kriegs, M.; Herges, R.; Peifer, C. Photoswitchable Azo- and Diazocine-Functionalized Derivatives of the VEGFR-2 Inhibitor Axitinib. *Int. J. Mol. Sci.* **2020**, *21* (23), 8961, 1-20.

(36) Thapaliya, E. R.; Zhao, J.; Ellis-Davies, G. C. R. Locked-Azobenzene: Testing the Scope of a Unique Photoswitchable Scaffold for Cell Physiology. *ACS Chem. Neurosci.* **2019**, *10* (5), 2481–2488.

(37) Trads, J. B.; Hüll, K.; Matsuura, B. S.; Laprell, L.; Fehrentz, T.; Görldt, N.; Kozek, K. A.; Weaver, C. D.; Klöcker, N.; Barber, D. M.; Trauner, D. Sign Inversion in Photopharmacology: Incorporation of Cyclic Azobenzenes in Photoswitchable Potassium Channel Blockers and Openers. *Angew. Chem. Int.Ed.***2019**, *58* (43), 15421–15428.

(38) Eljabu, F.; Dhruval, J.; Yan, H. Incorporation of cyclic azobenzene into oligodeoxynucleotides for the photo-regulation of DNA hybridization. *Bioorg. Med. Chem. Lett.* **2015**, *25* (23), 5594–5596.

(39) Preußke, N.; Moormann, W.; Bamberg, K.; Lipfert, M.; Herges, R.; Sönnichsen, F. D. Visible-light-driven photocontrol of the Trp-cage protein fold by a diazocine cross-linker. *Org. Biomol. Chem.* **2020**, *18* (14), 2650–2660.

(40) Reynders, M.; Chaikuad, A.; Berger, B.-T.; Bauer, K.; Koch, P.; Laufer, S.; Knapp, S.; Trauner, D. Controlling the Covalent Reactivity of a Kinase Inhibitor with Light. *Angew. Chem. Int. Ed.* **2021**, *60* (37), 20178–20183.

(41) Samanta, S.; Qin, C.; Lough, A. J.; Woolley, G. A. Bidirectional photocontrol of peptide conformation with a bridged azobenzene derivative. *Angew. Chem. Int. Ed.* **2012**, *51* (26), 6452–6455.

(42) Bieszczad, B.; Siwek, A.; Wilczek, M.; Trzybiński, D.; Woźniak, K.; Satała, G.; Bojarski, A. J.; Mieczkowski, A. Synthesis, crystal structure and biological activity of novel analogues of tricyclic drugs. *Bioorganic Med. Chem. Lett.* **2020**, *30* (21), 127493.

(43) Tsuchiya, K.; Umeno, T.; Tsuji, G.; Yokoo, H.; Tanaka, M.; Fukuhara, K.; Demizu, Y.; Misawa, T. Development of Photoswitchable Estrogen Receptor Ligands. *Chem. Pharm. Bull.* **2020**, *68* (4), 398–402.

(44) Morstein, J.; Awale, M.; Reymond, J.-L.; Trauner, D. Mapping the Azolog Space Enables the Optical Control of New Biological Targets. *ACS Cent. Sci.* **2019**, *5* (4), 607–618.

(45) Hinnah, K.; Willems, S.; Morstein, J.; Heering, J.; Hartrampf, F. W. W.; Broichhagen, J.; Leippe, P.; Merk, D.; Trauner, D. Photohormones Enable Optical Control of the Peroxisome Proliferator-Activated Receptor γ (PPARγ). *J. Med. Chem.* **2020**, *63* (19), 10908–10920.

(46) Brzozowski, A. M.; Pike, A. C.; Dauter, Z.; Hubbard, R. E.; Bonn, T.; Engström, O.; Ohman, L.; Greene, G. L.; Gustafsson, J. A.; Carlquist, M. Molecular basis of agonism and antagonism in the oestrogen receptor. *Nature* **1997**, *389* (6652), 753–758.

(47) Chaudhuri, N. K.; Ball, T. J. Synthesis of imipramine labelled with four deuterium atoms in 10, 11 positions. *J. Labelled Compd. Radiopharm.* **1981**, *18* (8), 1189–1196.

(48) Moormann, W.; Langbehn, D.; Herges, R. Solvent-Free Synthesis of Diazocine. *Synthesis* **2017**, *49* (15), 3471–3475.

(49) Moormann, W.; Langbehn, D.; Herges, R. Synthesis of functionalized diazocines for application as building blocks in photo- and mechanoresponsive materials. *Beilstein J. Org. Chem.* **2019**, *15*, 727–732.

(50) Fitjer, L.; Quabeck, U. The Wittig Reaction Using Potassium-tert-butoxide High Yield Methylenations of Sterically Hindered Ketones. *Synth. Commun.* **1985**, *15* (10), 855–864.

(51) Maier, M. S.; Hüll, K.; Reynders, M.; Matsuura, B. S.; Leippe, P.; Ko, T.; Schäffer, L.; Trauner, D. Oxidative Approach Enables Efficient Access to Cyclic Azobenzenes. *J. Am. Chem. Soc.* **2019**, *141* (43), 17295–17304.

(52) Ball, P.; Nicholls, C. H. Azo-hydrazone tautomerism of hydroxyazo compounds—a review. *Dyes Pigm.* **1982**, *3* (1), 5–26.

(53) Chen, X.-C.; Tao, T.; Wang, Y.-G.; Peng, Y.-X.; Huang, W.; Qian, H.-F. Azo-hydrazone tautomerism observed from UV-vis spectra by pH control and metal-ion complexation for two heterocyclic disperse yellow dyes. *Dalton Trans.* **2012**, *41* (36), 11107–11115.

(54) Gabor, G.; Frei, Y.; Gegiou, D.; Kaganowitch, M.; Fischer, E. Tautomerism and Geometric Isomerism in Arylazo-Phenols and Naphthols. Part III. Orthohydroxy Derivatives and their Reversible Photochemical Reactions. *Isr. J. Chem.* **1967**, *5* (5), 193–211.

(55) Dokić, J.; Gothe, M.; Wirth, J.; Peters, M. V.; Schwarz, J.; Hecht, S.; Saalfrank, P. Quantum chemical investigation of thermal cis-to-trans isomerization of azobenzene derivatives: substituent effects, solvent effects, and comparison to experimental data. *J. Phys. Chem. A* **2009**, *113* (24), 6763–6773.

(56) Cembran, A.; Bernardi, F.; Garavelli, M.; Gagliardi, L.; Orlandi, G. On the mechanism of the cis-trans isomerization in the lowest electronic states of azobenzene: S0, S1, and T1. *J. Am. Chem. Soc.* **2004**, *126* (10), 3234–3243.

(57) Schlimm, A.; Löw, R.; Rusch, T.; Röhricht, F.; Strunskus, T.; Tellkamp, T.; Sönnichsen, F.; Manthe, U.; Magnussen, O.; Tuczek, F.; Herges, R. Long-Distance Rate Acceleration by Bulk Gold. *Angew. Chem. Int. Ed.* **2019**, *58* (20), 6574–6578.

(58) Böckmann, M.; Doltsinis, N. L.; Marx, D. Unraveling a Chemically Enhanced Photoswitch: Bridged Azobenzene. *Angew. Chem. Int. Ed.* **2010**, *122* (19), 3454–3456.

(59) Jiang, C.-W.; Xie, R.-H.; Li, F.-L.; Allen, R. E. Comparative studies of the trans-cis photoisomerizations of azobenzene and a bridged azobenzene. *J. Phys. Chem. A* **2011**, *115* (3), 244–249.

(60) Muždalo, A.; Saalfrank, P.; Vreede, J.; Santer, M. Cis-to- Trans Isomerization of Azobenzene Derivatives Studied with Transition Path Sampling and Quantum Mechanical/Molecular Mechanical Molecular Dynamics. *J. Chem. Theory Comput.* **2018**, *14* (4), 2042–2051.

(61) Shinkai, S.; Nakaji, T.; Nishida, Y.; Ogawa, T.; Manabe, O. Photoresponsive crown ethers. 1. Cis-trans isomerism of azobenzene as a tool to enforce conformational changes of crown ethers and polymers. *J. Am. Chem. Soc.* **1980**, *102* (18), 5860–5865.

(62) Rau, H.; Lueddecke, E. On the rotation-inversion controversy on photoisomerization of azobenzenes. Experimental proof of inversion. *J. Am. Chem. Soc.* **1982**, *104* (6), 1616–1620.

(63) Kojima, M.; Nebashi, S.; Ogawa, K.; Kurita, N. Effect of solvent on cis -to- trans isomerization of 4-hydroxyazobenzene aggregated through intermolecular hydrogen bonds. *J. Phys. Org. Chem.* **2005**, *18* (10), 994–1000.

(64) Garcia-Amorós, J.; Sánchez-Ferrer, A.; Massad, W. A.; Nonell, S.; Velasco, D. Kinetic study of the fast thermal cis-to-trans isomerisation of para-, ortho- and polyhydroxyazobenzenes. *Phys. Chem. Chem. Phys.* **2010**, *12* (40), 13238–13242.

(65) Bell, L. R.; Truong, N. T. Primary and Solvent Kinetic Isotope Effects in the Water-Assisted Tautomerization of Formamidine: An ab Initio Direct Dynamics Study. *J. Phys. Chem. A* **1997**, *101*, 7802–7808.

(66) Mai, B. K.; Park, K.; Duong, M. P. T.; Kim, Y. Proton transfer dependence on hydrogen-bonding of solvent to the water wire: a theoretical study. *J. Phys. Chem. B* **2013**, *117* (1), 307–315.

(67) Peng, C. S.; Baiz, C. R.; Tokmakoff, A. Direct observation of ground-state lactam-lactim tautomerization using temperature-jump transient 2D IR spectroscopy. *PNAS* **2013**, *110* (23), 9243–9248.

(68) Singh, R.; Bharti, N.; Madan, J.; Hiremath, S. N., J. Characterization of Cyclodextrin Inclusion Complexes. *Pharm. Sci. Technol. Today* **2010**, *2*, 171–183.

(69) Kfoury, M.; Landy, D.; Fourmentin, S. Characterization of Cyclodextrin/Volatile Inclusion Complexes: A Review. *Molecules* **2018**, *23* (5), 1204, 1-23.

(70) Crini, G. Review: a history of cyclodextrins. *Chem. Rev.* **2014**, *114* (21), 10940-10975.

(71) Bannwarth, C.; Caldeweyher, E.; Ehlert, S.; Hansen, A.; Pracht, P.; Seibert, J.; Spicher, S.; Grimme, S. Extended tight-binding quantum chemistry methods. *WIREs Comput. Mol. Sci.* **2021**, *11* (2), 1-49.

(72) Bannwarth, C.; Ehlert, S.; Grimme, S. GFN2-xTB-An Accurate and Broadly Parametrized Self-Consistent Tight-Binding Quantum Chemical Method with Multipole Electrostatics and Density-Dependent Dispersion Contributions. *J. Chem. Theory Comput.* **2019**, *15* (3), 1652–1671.

(73) Grimme, S.; Antony, J.; Ehrlich, S.; Krieg, H. A consistent and accurate ab initio parametrization of density functional dispersion correction (DFT-D) for the 94 elements H-Pu. *J. Chem. Phys.* **2010**, *132* (15), 154104.

(74) Lin, Y.-S.; Li, G.-D.; Mao, S.-P.; Chai, J.-D. Long-Range Corrected Hybrid Density Functionals with Improved Dispersion Corrections. *J. Chem. Theory Comput.* **2013**, *9* (1), 263–272.

(75) Neese, F.; Wennmohs, F.; Becker, U.; Riplinger, C. The ORCA quantum chemistry program package. *J. Chem. Phys.* **2020**, *152* (22), 224108.

(76) Neese, F.; Wennmohs, F.; Hansen, A.; Becker, U. Efficient, approximate and parallel Hartree–Fock and hybrid DFT calculations. A 'chain-of-spheres' algorithm for the Hartree–Fock exchange. *Chem. Phys.* **2009**, *356* (1-3), 98–109.

(77) Weigend, F. Accurate Coulomb-fitting basis sets for H to Rn. *Phys. Chem. Chem. Phys.* **2006**, *8* (9), 1057–1065.

(78) Weigend, F.; Ahlrichs, R. Balanced basis sets of split valence, triple zeta valence and quadruple zeta valence quality for H to Rn: Design and assessment of accuracy. *Phys. Chem. Chem. Phys.* **2005**, *7* (18), 3297–3305.

(79) Hall, J. M.; McDonnell, D. P. The estrogen receptor beta-isoform (ERbeta) of the human estrogen receptor modulates ERalpha transcriptional activity and is a key regulator of the cellular response to estrogens and antiestrogens. *Endocrinology* **1999**, *140* (12), 5566–5578.

(80) Hall, J. M.; Korach, K. S. Analysis of the molecular mechanisms of human estrogen receptors alpha and beta reveals differential specificity in target promoter regulation by xenoestrogens. *J. Biol. Chem.* **2002**, *277* (46), 44455–44461.

(81) Kuznetsov, Y. V.; Levina, I. S.; Scherbakov, A. M.; Andreeva, O. E.; Fedyushkina, I. V.; Dmitrenok, A. S.; Shashkov, A. S.; Zavarzin, I. V. New estrogen receptor antagonists. 3,20-Dihydroxy-19-norpregna-1,3,5(10)-trienes: Synthesis, molecular modeling, and biological evaluation. *Eur. J. Med. Chem.* **2018**, *143*, 670–682.

(82) Kwon, J.; Oh, K. S.; Cho, S.-Y.; Bang, M. A.; Kim, H. S.; Vaidya, B.; Kim, D. Estrogenic Activity of Hyperforin in MCF-7 Human Breast Cancer Cells Transfected with Estrogen Receptor. *Planta Med.* **2016**, *82* (16), 1425–1430.

(83) Sun, H.; Xu, X.-L.; Qu, J.-H.; Hong, X.; Wang, Y.-B.; Xu, L.-C.; Wang, X.-R. 4-Alkylphenols and related chemicals show similar effect on the function of human and rat estrogen receptor alpha in reporter gene assay. *Chemosphere* **2008**, *71* (3), 582–588.

(84) van den Belt, K.; Berckmans, P.; Vangenechten, C.; Verheyen, R.; Witters, H. Comparative study on the in vitro/in vivo estrogenic potencies of 17beta-estradiol, estrone, 17alpha-ethynylestradiol and nonylphenol. *Aquat. Toxicol.* **2004**, *66* (2), 183–195.

(85) Druckrey, H.; Danneberg, P.; Schmaehl, D. Ein oestrogener Azo-Farbstoff. *Zeitschrift für Naturforschung B* **1950**, *5* (1), 27–28.

(86) Boström, J.; Norrby, P. O.; Liljefors, T. Conformational energy penalties of protein-bound ligands. *J. Comput. Aided Mol. Des.* **1998**, *12* (4), 383–396.

(87) Nicklaus, M. C.; Wang, S.; Driscoll, J. S.; Milne, G. W. Conformational changes of small molecules binding to proteins. *Bioorg. Med. Chem.* **1995**, *3* (4), 411–428.

(88) Vieth, M.; Hirst, J. D.; Brooks, C. L. Do active site conformations of small ligands correspond to low free-energy solution structures? *J. Comput. Aided Mol. Des.* **1998**, *12* (6), 563–572.

(89) Müller-Deku, A.; Meiring, J. C. M.; Loy, K.; Kraus, Y.; Heise, C.; Bingham, R.; Jansen, K. I.; Qu, X.; Bartolini, F.; Kapitein, L. C.; Akhmanova, A.; Ahlfeld, J.; Trauner, D.; Thorn-Seshold, O. Photoswitchable paclitaxel-based microtubule stabilisers allow optical control over the microtubule cytoskeleton. *Nat. Commun.* **2020**, *11* (1), 4640.

(90) Sailer, A.; Ermer, F.; Kraus, Y.; Bingham, R.; Lutter, F. H.; Ahlfeld, J.; Thorn-Seshold, O. Potent hemithioindigo-based antimitotics photocontrol the microtubule cytoskeleton in cellulo. *Beilstein J. Org. Chem.* **2020**, *16*, 125–134.

(91) Prischich, D.; Gomila, A. M. J.; Milla-Navarro, S.; Sangüesa, G.; Diez-Alarcia, R.; Preda, B.; Matera, C.; Batlle, M.; Ramírez, L.; Giralt, E.; Hernando, J.; Guasch, E.; Meana, J. J.; La Villa, P. de; Gorostiza, P. Adrenergic Modulation With Photochromic Ligands. *Angew. Chem. Int. Ed.* **2021**, *60* (7), 3625–3631.

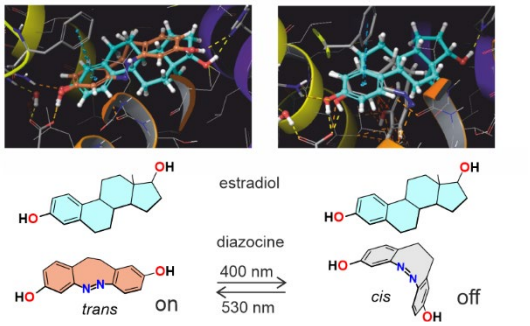
estradiol
diazocine
400 nm
530 nm
trans
on
cis
off